ELSEVIER

Journal of Hydrology 268 (2002) 214–233

Journal of Hydrology

www.elsevier.com/locate/jhydrol

Numerical simulation of unsaturated flow along preferential pathways: implications for the use of mass balance calculations for isotope storm hydrograph separation

S.J. Van der Hoven[a,*], D.K. Solomon[b], G.R. Moline[c]

[a]*Department of Geography–Geology, Illinois State University, Normal, IL 61701-4400, USA*
[b]*Department of Geology and Geophysics, University of Utah, Salt Lake City, UT 84112-0111, USA*
[c]*Environmental Sciences Division, Oak Ridge National Laboratory, Oak Ridge, TN 37831-6038, USA*

Received 22 May 2001; revised 5 June 2002; accepted 5 July 2002

Abstract

An objective common to many watershed studies is to separate storm hydrographs into two components: water that was present in the watershed prior to a storm event (soil moisture and groundwater) and water which fell on the watershed during the storm. To use this approach, a number of assumptions must be made including that the composition of water in the soil moisture and groundwater reservoirs are constant and known. The objective of this paper is to show that in settings where flow and transport are dominated by preferential pathways for flow, steady state mass balance calculations for quantitative hydrograph separation may be in error. We present field data from a site where flow and transport are dominated by preferential pathways (relict fractures in saprolite of sedimentary rocks) which indicate that the $\delta^{18}O$ content of the water in the unsaturated and shallow saturated zones is not constant over the course of a storm event. We use a numerical model to further explore the interactions between the fractures and surrounding matrix. Both the field data and modeling results indicate that the $\delta^{18}O$ of the previous storm event(s) has a strong influence on water in the fractures. On the time scale of a storm event, only the water in the matrix immediately surrounding the fracture mixes with water in the fracture, while the bulk of the matrix is isolated from fracture flow. The spatial and temporal heterogeneity of the $\delta^{18}O$ in the subsurface and the isolation of the most of the matrix water from flow in fractures make the measurement of a singular $\delta^{18}O$ value for subsurface reservoirs problematic and the assumption of a constant value doubtful. Since most near-surface geologic materials have preferential flow paths, we suggest that quantitative hydrograph separation using mass balance techniques is not possible in most situations. Future field and modeling investigations using the approach outlined here could be designed to explore the important temporal and spatial scales of variability in watersheds, and lead to a more quantitative approach to storm hydrograph separation.

Keywords: Stable isotopes; Hydrographs; Preferential flow; Saprolite; Numerical model; Unsaturated zone

1. Introduction

A common question in watershed studies is to determine to origin of the increased stream discharge during precipitation events. Is the increased discharge

* Corresponding author.
E-mail address: sjvande2@ilstu.edu (S.J. Van der Hoven).

0022-1694/02/$ - see front matter
PII: S0022-1694(02)00178-6

from water which was present in the watershed prior to a storm event (pre-event or old water), water, which fell on the watershed during a storm (event or new water) or some combination of the two? Mass balance equations are frequently used to answer this question. In their simplest form, the mass balance equations are:

$$Q_s = Q_n + Q_o \quad (1)$$

and

$$Q_s C_s = Q_n C_n + Q_o C_o \quad (2)$$

where Q is discharge, C is concentration of a tracer, and the subscripts s, n, and o are streamflow, event water, and pre-event water, respectively. In this form, the pre-event water is assumed to be groundwater from the saturated zone. However, some investigators have subdivided pre-event water into components from the unsaturated and saturated zones (DeWalle et al., 1988; O'Brien and Hendershot, 1993). The contribution of each component is determined by monitoring a natural environmental tracer that has a signal characteristic to that component. Commonly used environmental tracers include isotopes of hydrogen and oxygen, dissolved ions including Na, Ca, Al, Cl, Fl, and Si, and specific conductance (Pinder and Jones, 1969; Sklash and Farvolden, 1979; Pilgram et al., 1979).

Hydrograph separation techniques, which use mass balance of environmental tracers, require a number of assumptions (Sklash and Farvolden, 1982). They include:

(1) Groundwater and baseflow can be characterized by a single constant composition.
(2) Rain or snowmelt can be characterized by a single constant composition. If this is not the case, the variations in composition are documented.
(3) The composition of rain water is significantly different from that of groundwater/baseflow.
(4) Contributions from soil water are negligible, or the composition is identical to that of groundwater.
(5) Contributions from surface water bodies are negligible.

The validity of these assumptions has been questioned by some researchers. Stewart and McDonnell (1991) monitored variations in deuterium in precipitation, soil water and groundwater for a period of several months. They found significant variability which lagged in comparison to that of the precipitation, and which decreased with depth. They also concluded that much of the rainfall bypassed the soil matrix while advectively mixing with the matrix surrounding macropores and cracks. Kendall and McDonnell (1993) summarize a number of investigations which demonstrate spatial and temporal variability in precipitation, soil water, and groundwater. Elsenbeer et al. (1994) monitored the water chemistry in a tropical rainforest setting and conclude that their data do not support temporal invariance of end members.

The recognition of temporal variations has lead to the development of methods to account for the variability. Harris et al. (1995) proposed a hydrograph separation approach based on mass balance that continuously varies the composition and size of each reservoir. Genereux (1998) explored a method to quantify the component uncertainty in hydrograph separation of two and three component systems based on the application of general uncertainty propagation. For two component systems, the uncertainly was found to decrease as the difference in concentration between the components increased. The uncertainty was also found to be more sensitive to the component that made up more that half of the mixture, which for many studies has been found to be the 'old' water. An example of a three component system indicates that the uncertainly analysis is dependent on the mixing fractions, which change through time.

While it is evident that there is significant variability in the composition of subsurface reservoirs, most hydrograph separation studies reported in the literature do not consider potential spatial and temporal variability in individual components. The study described in this paper was originally designed to evaluate spatial and temporal variations in the vadose zone and shallow groundwater, not as a test of the hydrograph separation technique on a catchment scale. However, during the course of the field investigation and subsequent vadose zone numerical modeling, the potential impacts on storm hydrograph separation using chemical or isotopic techniques were noted. A relatively simple numerical simulation was

designed to illustrate pore-scale interactions that may affect the assumptions of hydrograph separation. The objective of this paper is to show that in settings where flow and transport are dominated by preferential pathways for flow, steady state mass balance calculations for quantitative hydrograph separation may be in error by assuming a constant composition for subsurface reservoirs. To our knowledge, vadose zone transport modeling that includes preferential flow paths has not been used to address the problem of variability in the composition of subsurface reservoir during storm hydrograph separation.

2. Study area

This study was conducted on the Oak Ridge Reservation (ORR) in eastern Tennessee, USA. It is underlain by Cambrian and Ordovician age sedimentary rocks, primarily shale and limestone/dolomite. The bedrock units are repeated across the ORR in a series of imbricate thrust sheets. Beneath the study area, bedrock dips at around 45° to the southeast. Differential erosion of the various geologic units results in a parallel ridges and valleys. Elevations range from 250 m in the valleys to 330 m on the ridges. Average precipitation is 120 cm/yr, with somewhat greater amounts falling in the winter and spring than in summer and fall. The main streams run parallel to the ridges and tributaries crosscut the valley floor at an angle.

Numerous investigations of flow and transport in the vadose zone have been conducted on the ORR. The soils and saprolite (highly weathered bedrock) are characterized by a continuous distribution of pore sizes. However, for classification purposes Luxmoore (1981) defined three pore classes: macropores (>1 mm pore diameter), mesopores (between 1 and 0.1 mm pore diameter), and micropores (<0.1 mm pore diameter). Watson and Luxmoore (1986) found that the macropores (0.04% of the soil volume) could transmit 76% of the water flux during saturated conditions and that 96% of the water flux could be transmitted through macro and mesopores (0.32% of the soil volume). At field capacity, the macro- and mesopores are drained, while the micropores remain saturated (Luxmoore et al., 1990). Wilson et al. (1990) found that preferential flow through macro- and mesopores occurred in subsurface of a forested hillslope when perched water table conditions were present as well as during dry conditions due to hydrophobicity. Intermediate soil water conditions resulted in minimal preferential flow due to infiltration into soil matrix pores. Wilson et al. (1990) conclude that preferential flow from hillslopes is the predominant subsurface flow mechanism.

Both Luxmoore et al. (1990) and Wilson et al. (1991b) used patterns in the concentration of major ions dissolved in subsurface flow during storm events to infer transport process in the different pore classes. The most common pattern for water in larger pores was an increase in concentration as flow increased and a decrease in concentration on the recession limb of the subsurface hydrograph. Wilson et al. (1991b) summarize the conceptual model of transport in the vadose zone during storm events. Prior to a storm event, only the micropores are saturated. As precipitation infiltrates, it initially causes saturation in mesopores. Solute concentrations in the mesopores are initially low due to dominance of low concentration precipitation. As more mesopores become hydraulically active, there is greater surface area interaction with micropores that have higher solute concentrations. Because of increasing soil air pressure, advective exchange of solutes occurs between micropores and mesopores. If subsurface flow increases further, micro- and mesopores contribute water with relatively high concentrations of solutes to macropore flow. As flow decreases, solute concentrations in larger pores decrease because the increasingly small volume of hydraulically active pores has already been flushed of solutes. Contributions of solutes from micropores also decrease because the dominant transport mechanism between micropores and larger pores changes from advection to diffusion. The concentration of solutes in the bulk of micropores was found to be constant over the course of a storm event and therefore they concluded that micropores were a semi-infinite source of solutes to the larger pores.

A buried line source tracer test reported by Wilson et al. (1993) provided further insight into preferential flow and transport in the vadose zone of the ORR. Rapid transport through macro- and mesopores was observed. During one injection, the tracer was detected 65 m from the source 3.2 h after the start of

injection. Initially, micropores served as a sink for the tracer, but through time, their role reversed, as micropores became a source for the tracer in the larger pores sizes. The patterns of tracer concentration over the course of storm events were similar to those observed in major ions by Luxmoore et al. (1990) and Wilson et al. (1991b). The use of an injected tracer showed that the dominant transport direction was along geologic strike rather than following the topographic slope. This observation illustrated the importance of bedding plane fractures as preferential pathways for flow in this setting.

Storm hydrograph separation studies have been performed in Walker Branch watershed on the ORR. Walker Branch is a few kilometers from the Bear Creek Valley site used during this investigation. The two sites have similar flow and transport processes in the shallow subsurface. One main difference is that the bedrock underlying Walker Branch is dolomite and has karst flow, while the Bear Creek Valley site is underlain by shale with no karst flow. Mulholland et al. (1990) describe hydrograph separation for several storm events using calcium to separate two subsurface components of storm flow generation. The two components were shallow flow within the soil profile and deep flow within the bedrock. The calcium concentration for the shallow component was a mean flow-proportional concentration for an ephemeral stream in the upper part of the watershed. The concentration in a perennial spring during base flow conditions was used to represent deep bedrock flow. The percentage of the two components was found to vary in space and time, with the shallow flow path dominating in the upper part of the watershed and the deep flow path dominating in the lower part of the watershed. They also concluded that large percentage of the watershed (including hillslopes and ridges) was contributing to stream flow during storms by flow along preferential pathways (large pores) in soils.

Mulholland (1993) refined the previous storm hydrograph studies in Walker Branch watershed using calcium and sulfate and three subsurface components: vadose zone, saturated soil, and deep bedrock flow. The concentrations of calcium and sulfate for each component were defined as: the mean concentrations during the storm from a subsurface weir collecting perched, saturated flow from the vadose zone; mean concentrations over a 6 month period from a well in the saturated soil; and concentrations from a perennial spring at baseflow prior to the storm. The conclusion of this study was that large increases in stream flow during storms were a "result of development of perched water tables in upper soil layers in the catchment, which in turn initiate rapid preferential flow along shallow and relatively deep flowpaths through soils". Although the relative age of water in the different flow components was not addressed, Wilson et al. (1991a) concluded that 30–50% of the vadose zone flow was old water based on electrical conductivity measurements in the subsurface weir during storm events.

Genereux et al. (1993) investigated stream flow generation over a wide range of flow conditions in Walker Branch watershed using ^{222}Rn and calcium as tracers for three subsurface components: vadose zone, saturated soil, and deep bedrock flow. The fraction of water from each component contributing to stream flow is calculated using a single averaged concentration for each component. A part of this investigation included evaluation of the spatial and temporal variability in concentration of the three components. To address temporal variability, samples were collected on a daily to monthly basis, and to address spatial variability, samples were collected on a scale of meters to kilometers. Although considerable variability was found in the vadose zone and saturated soil components, the concentration difference between these three components was large enough that the averaged concentrations were deemed useful for mixing calculations. Their data indicate a potential for seasonal variations in tracer concentration, but the sampling resolution is not high enough to include seasonal variations in mixing calculations. They state that seasonal variations in component tracer concentrations could be addressed by data sets with finer spatial and temporal resolution.

During the investigation reported here, samples were collected from two different sites within the study area. The first site was located on the gently sloping valley floor, approximately 300 m from the closest perennial stream (Fig. 1). The second site is located adjacent to one of the tributary streams, at the base of a slope approximately 15 m from the floodplain of the stream (Fig. 2). The soils at both sites have been classified as ruptic ultic dystrochrepts and are 50–60 cm thick (Watkins et al., 1993). Soil

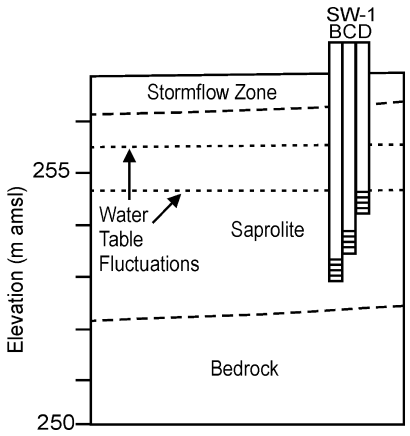

Fig. 1. Hydrogeologic cross-section for the site away from a stream showing the shallow hydrogeologic units, water table fluctuations during the storm event and screened intervals of the multiport well.

development has created an intermittently saturated zone in the near-surface known as the stormflow zone. Throughout this paper, stormflow refers to the transient perched saturated zone that develops in the upper soil horizons during some precipitation events. The permeability of the near-surface soil A horizon is much greater than the Bt horizon and saprolitic C horizon. The infiltration rate of the A horizon is high enough to accommodate all but the highest precipitation rates, however, water becomes perched on the lower permeability Bt horizon and saprolite (Solomon et al., 1992; McKay and Driese, 1999). Saprolite, the highly weathered remnant of the shale and limestone bedrock, underlies the soils. The saprolite retains some important characteristics of unweathered bedrock, including bedding plane structures and fractures. Dissolution of primary minerals and precipitation of secondary minerals during weathering has resulted in a porosity change from $<5\%$ in unweathered bedrock to $>40\%$ in the saprolite.

Both sites are located in groundwater discharge zones. During non-storm periods, evidence from hydraulic measurements, major ion chemistry, and dissolved gases indicates that there is an upward vertical flux of water (Van der Hoven, 2000). Data from nested piezometers at a number of sites within the study area indicate that water discharging vertically upward has high total dissolved solids and high sodium (Na) concentration. Numerous samples of groundwater at depths of between 10 and 20 m below the water table have a relatively constant $\delta^{18}O$ of -5.8 to $-6.0‰$. During storm events, the large flux of water through the unsaturated zone reverses the hydraulic gradient in the shallow saturated zone. The water recharging through the unsaturated zone has low Na concentration and variable $\delta^{18}O$ content.

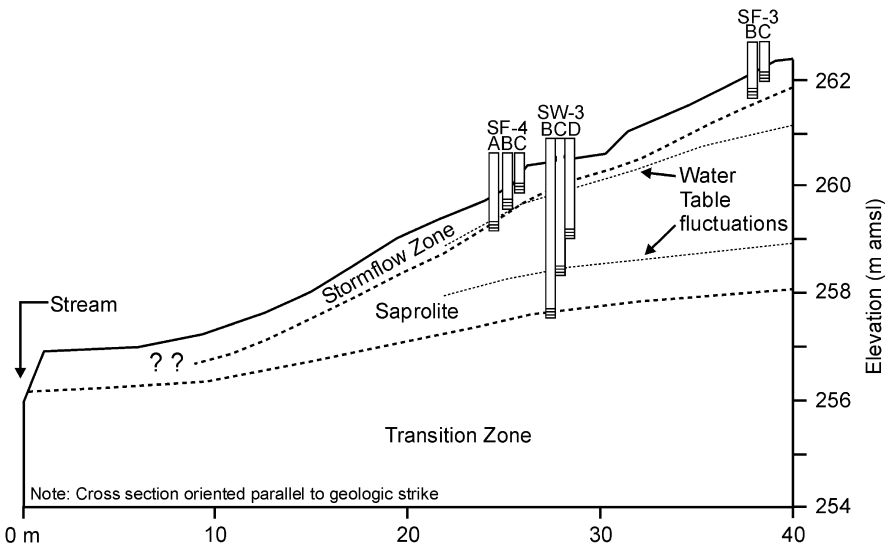

Fig. 2. Hydrogeologic cross-section for the site adjacent to a stream showing the shallow hydrogeologic units, water table fluctuations during the storm event, stormflow tubes, and screened intervals of the multiport well.

3. Methodology

Samples were collected from two storm events; in January and April–May 1998. During each event, water samples were collected from precipitation, the stormflow zone and shallow groundwater within the saprolite. Direct precipitation samples were collected using a 40-cm diameter polyethylene funnel and a 2 l polyethylene bottle. Bulk precipitation samples were collected every 6–12 h. A 30-ml aliquot was taken from each bulk sample, stored in a glass vial with a teflon-lined lid, and kept refrigerated until analysis. Precipitation rate was measured using an automatic tipping bucket gauge set to record measurements every 15 min.

Water from the stormflow zone during periods of saturation was collected from stormflow tubes. Stormflow tubes were constructed by hand auguring a 9-cm diameter hole to the desired depth. A 13-cm length of 2-cm ID PVC screen was placed at the bottom of the hole, and blank casing extended above the surface. The annular space around the screen was backfilled with sand and the remainder of the annular space was filled with compacted soil. Water samples were collected using a peristaltic pump, stored in 30-ml glass vials with a teflon-lined lid, and kept refrigerated until analysis.

Water from the saturated saprolite was collected from multiport wells. A 20-cm diameter borehole was drilled using a trailer-mounted hollow stem augur. During drilling, continuous cores were collected using Shelby tubes and screen depths were selected based on field analysis of the cores. Multiple sampling ports were installed in each borehole. Each port was constructed of 2 cm ID polyethylene tubing with a 10 cm length of screen constructed of wrapped wire mesh. Approximately 30 cm of the annular space straddling each port was filled with sand and the ports were isolated from each other by filling the annular space with bentonite. Approximately one well volume was purged prior to sampling and the purge rate was kept low in order to minimize the potential for inducing artificial hydraulic gradients. Water samples were collected using a peristaltic pump, stored in 30 ml glass vials with a teflon-lined lid, and kept refrigerated until analysis.

Na analyses were performed at Oak Ridge National Laboratory, Chemical and Analytical Division using a Thermo Jarrell Ash IRIS ICAP. The analytical uncertainty of the measurement was 0.2 mg/l. Oxygen isotopic analyses were performed at the University of Tennessee, Department of Geologic Sciences on a Finnagan Delta Plus gas source mass spectrometer with a HDO Equilibrator for automated analysis of water samples. The analytical uncertainty of the measurement was 0.1‰.

4. Results

4.1. January, 1998 storm event

During the January, 1998 storm event, samples were collected of precipitation, from the SF-4 stormflow tubes and from the SW-3 saturated saprolite in wells. The concentration of Na in the stormflow zone and saturated saprolite over the course of the storm event (Fig. 3) is representative of patterns for other major ions. Saturated conditions develop in the shallowest stormflow tube on Julian Day 6 after two periods of light rain in the previous 24 h (Fig. 3(b)). Saturation of a second stormflow tube begins about 6 h after the start of the main precipitation event on Day 7. The concentration pattern for both stormflow tubes is initially higher concentration that decreases to the concentration of Na in precipitation, and then increases slightly after the event is over. This pattern in major ions is consistent with the observations of Luxmoore et al. (1990) and Wilson et al. (1991a,b) and suggests that their conceptual model of unsaturated zone transport on the ORR is an appropriate model for the current investigation.

In the saturated saprolite (Fig. 3(c)), there is a positive correlation between Na and depth throughout the monitoring period. This concentration increase with depth is interpreted as a mixing zone between the high Na concentration water from depth discharging vertically and the low Na concentration water recharging at the water table. While the vertical pattern remains constant, the actual concentrations do not. All three wells show a decreasing concentration during the storm event, followed by a gradual increase over the next 7 days back to pre-storm concentrations. The variable recharge flux causes vertical migration of the mixing zone. During the heart of the storm, the concentration of Na in the two upper saprolite wells is

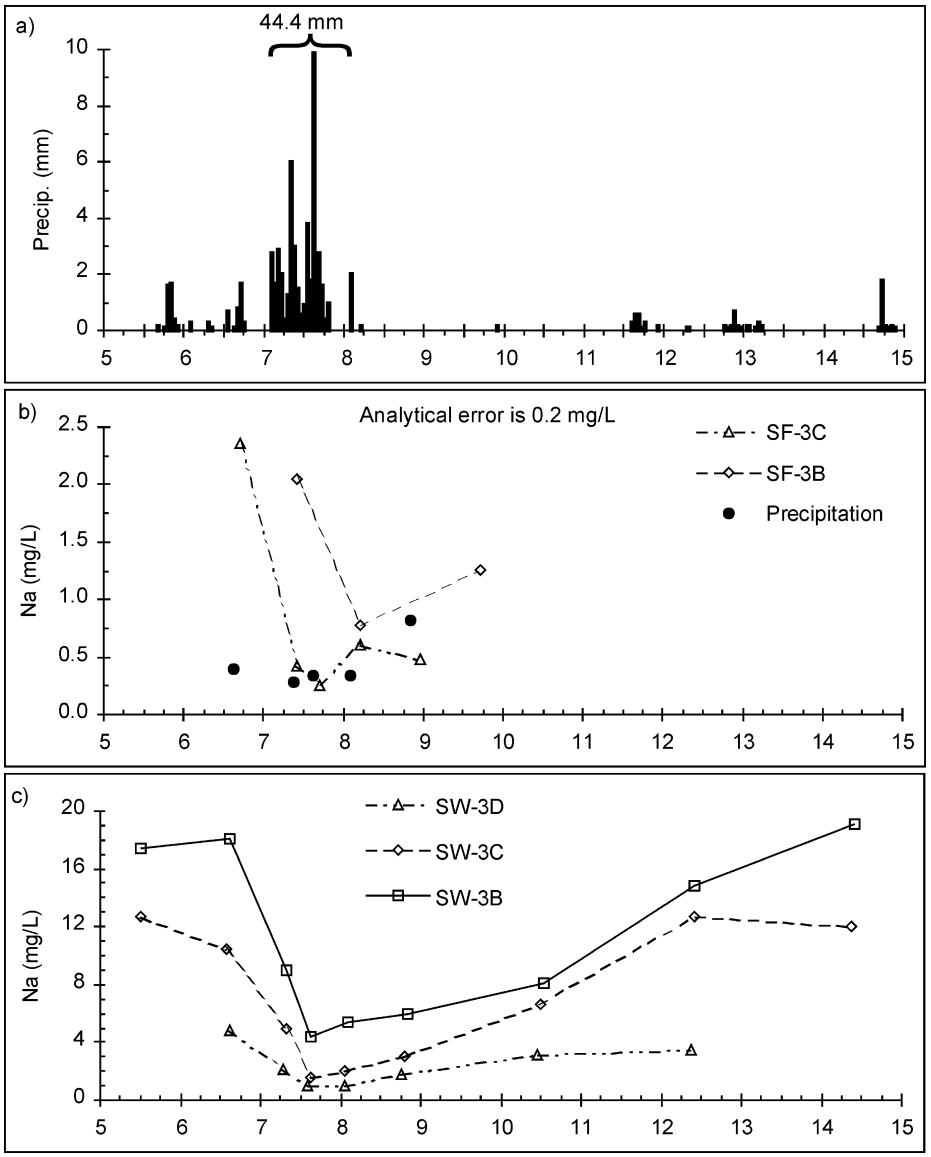

Fig. 3. Variations in Na concentration in the stormflow zone and shallow groundwater for a storm event in January, 1998. (a) Precipitation falling during the storm event in mm. (b) The Na concentration in the stormflow zone decreases as macropores are flushed of solutes by precipitation. (c) The Na concentration in the saturated saprolite decreases as recharging precipitation reverses the hydraulic gradient and replaces higher Na water that is discharging from depth.

similar to the Na concentrations in the stormflow tubes, supporting the concept of rapid transport along preferential pathways (bedding plane fractures) in both the unsaturated and saturated zones.

Fig. 4 presents variations in $\delta^{18}O$ over the course of the storm event. Prior to the monitoring period, several inches of snow fell over New Years and had melted by Day 2. Since this snowstorm was not sampled, its $\delta^{18}O$ is unknown. However, isotopic fractionation increases with decreasing temperature, and snow is generally isotopically more negative than rain for a given location. Saturation of the shallowest stormflow tube begins after the second small rain event on Day 6, indicating near saturation conditions

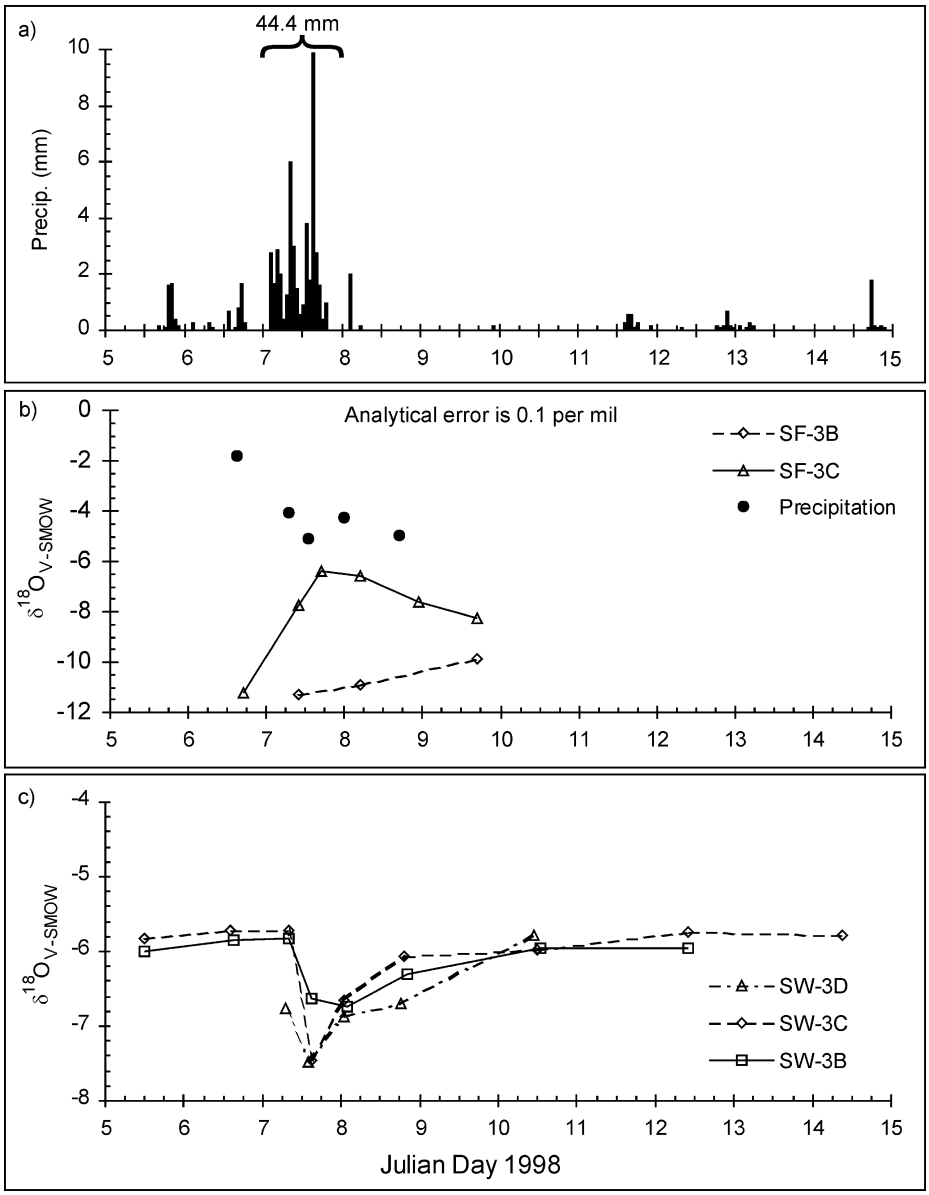

Fig. 4. Variations in $\delta^{18}O$ in the stormflow zone and shallow groundwater for a storm event in January, 1998. (a) Precipitation falling during the storm event in mm. (b) The $\delta^{18}O$ of water in the stormflow zone is initial isotopically light, reflecting the snow that fell the previous week, and becomes heavier as the new precipitation flushes out the hydraulically active pores. (c) Water from the stormflow zone is transported along preferential pathways in the unsaturated and saturated zones, as reflected by the decrease in $\delta^{18}O$ during precipitation.

the previous day. The initial $\delta^{18}O$ of water in all the stormflow tubes is 6–10‰ more negative than the $\delta^{18}O$ of precipitation (Fig. 4(b)). In the shallowest stormflow tube, the $\delta^{18}O$ increases to a value close to that of precipitation before decreasing again. This pattern is similar to that of Na, where concentration is initially different from the precipitation, subsequently approaching the value of precipitation, and finally concentrations moving back towards initial values. In the other stormflow tube, the $\delta^{18}O$ increases slightly over the monitoring period, but remains well below the $\delta^{18}O$ of precipitation.

In the saturated zone, the $\delta^{18}O$ prior to the storm event is constant at about $-6‰$ due an upward flux of water (Fig. 4(c)). The response to the precipitation starting on Day 7 is seen in the shallow groundwater within 6–12 h. The $\delta^{18}O$ of water in the saturated zone decreases significantly and is similar to water in the stormflow zone, indicating advective transport along preferential pathways in both the unsaturated and shallow saturated zones. The $\delta^{18}O$ in the saturated zone gradually increases over the rest of the monitoring period and returns to the pre-storm values. We interpret this to be a return to an upward flow of water with a constant $\delta^{18}O$ of about $-6.0‰$ and diffusion of water out of the saprolite matrix, also with a $\delta^{18}O$ of about $-6.0‰$.

4.2. April–May, 1998 storm event

During the April–May, 1998 storm event, samples were collected from the SF-3 stormflow tubes and from the SW-1 and SW-3 saturated saprolite wells. The SW-1 borehole is located approximately 300 m from a perennial stream and the thickness of unsaturated saprolite is at least 1 m greater than at SW-3.

The concentration of Na in the stormflow tubes (Fig. 5(b)) remains relatively constant throughout most of the monitoring period and is greater than the concentration in precipitation. It is difficult to make any interpretations of transport processes in the stormflow zone with these data. The intensity of precipitation during this event is less than the January event, and nearby tensiometer data indicate that relative saturation was less prior to the April–May event. This may have resulted in what Wilson et al. (1991a,b) call 'intermediate conditions' where preferential flow is minimal and mixing of precipitation with the matrix pores may be greater.

Na concentrations in the saturated saprolite (Fig. 5(c) and (d)) indicate that there is preferential flow through the unsaturated saprolite beneath the stormflow zone. Both sets of multiport wells show a vertical concentration gradient that is maintained throughout the monitoring period. Almost all wells show a decrease in the Na concentration during the main period of precipitation on Day 120. The decrease in the SW-1 wells, where the unsaturated saprolite is 1 m thicker, is subdued and lagged in comparison to the response in the SW-3 wells.

With the exception of SF-4A, there are only minor variations in the $\delta^{18}O$ of water in the stormflow zone over the period of saturation (Fig. 6(b)). The smaller variations in $\delta^{18}O$ in the stormflow zone during this storm event compared to the January, 1998 event may be due to several factors. In addition to the intermediate conditions discussed earlier, there may have been only a small difference between the isotopic composition of pre-event water and precipitation. The $\delta^{18}O$ composition of the pre-event water was not sampled; however, the absence of a dramatic change in the $\delta^{18}O$ content in the early part of the storm is an indication that the isotopic difference between the pre-event and event water was not as large as in the January storm event.

There is a significant $\delta^{18}O$ response in the saturated saprolite to the precipitation signal in both sets of multiport wells (Fig. 6(c) and (d)). In SW-1, only the port closest to the water table (SW-1D) shows a response to the storm event, and the response is delayed more than a day after the start of precipitation. However, the $\delta^{18}O$ in SW-1D is close to the value in the stormflow zone, suggesting preferential flow through the unsaturated saprolite. In SW-3, all three ports respond to the precipitation in less than a day. SW-3D responds within a few hours of the start of precipitation and has a $\delta^{18}O$ nearly identical to the stormflow zone. The response in SW-3B and SW-3C lags behind by 12 h and the increase is not as dramatic. The differences in response between the ports are thought to be due to mixing within the fractures and/or diffusive exchange between the fractures and matrix. The gradual decrease back to the pre-storm $\delta^{18}O$ over the course of the next several days is interpreted to be due to a return to an upward vertical

Fig. 5. Variations in Na concentration in the stormflow zone and shallow groundwater for a storm event in April–May, 1998. (a) Precipitation falling during the storm event in mm. (b) The concentration of Na in the stormflow zone remains constant throughout the monitoring period, but is higher than the concentration in precipitation. (c) The Na concentration in the saturated saprolite at SW-1 shows a subdued and lagged response to the precipitation. (d) The Na concentration in the saturated saprolite at SW-3 shows a large and rapid response to the precipitation.

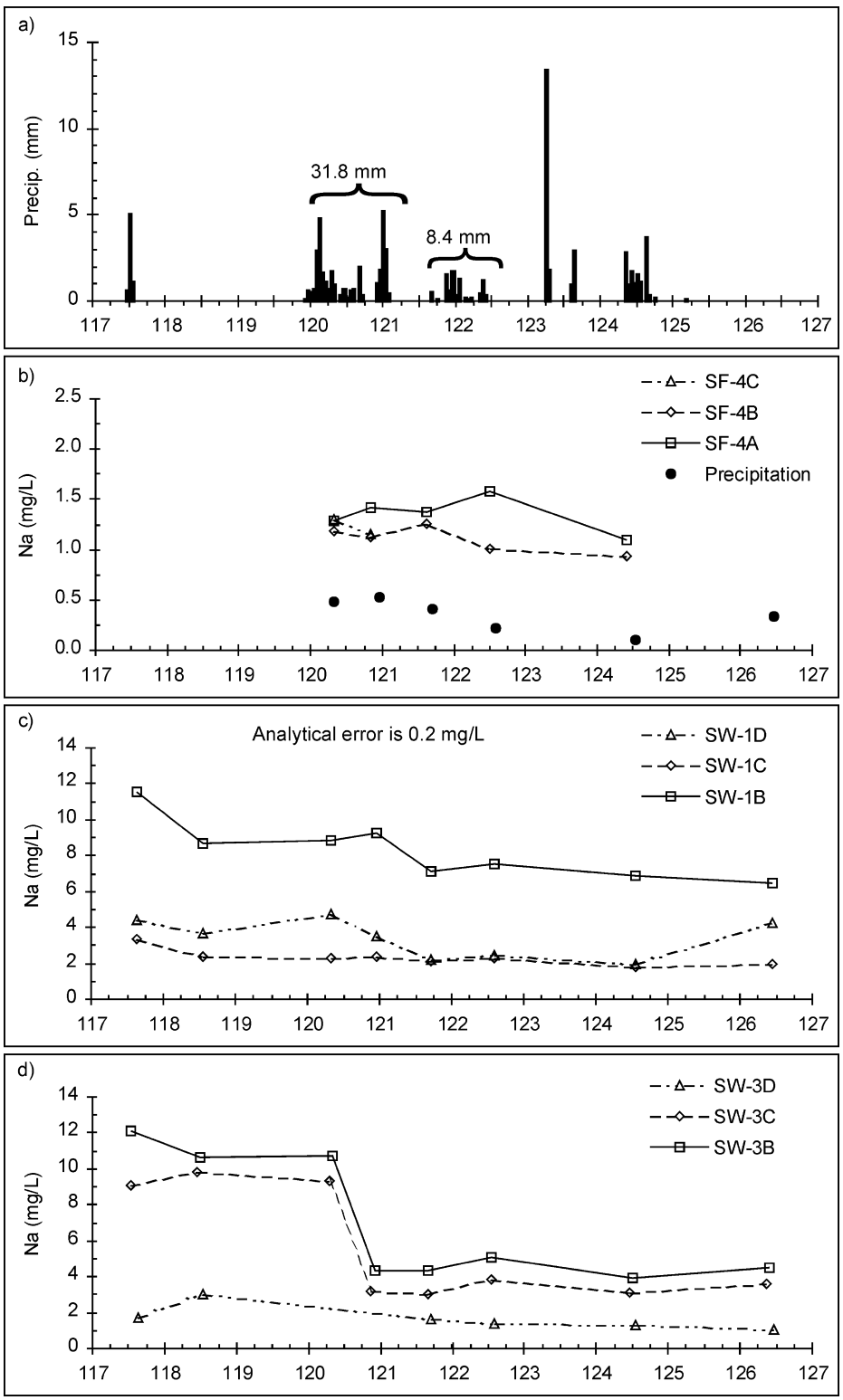
a)
Precip. (mm)
31.8 mm
8.4 mm
b)
Na (mg/L)
SF-4C
SF-4B
SF-4A
Precipitation
c)
Analytical error is 0.2 mg/L
Na (mg/L)
SW-1D
SW-1C
SW-1B
d)
Na (mg/L)
SW-3D
SW-3C
SW-3B

flux of water and/or recharge of isotopically lighter precipitation that fell during that period.

4.3. Numerical model

The conceptual model for flow and transport outlined in the previous sections was developed from the data collected during this study as well as numerous other investigations conducted on the ORR. In order to test some of the ideas of the conceptual model and explore in detail the flow and transport interactions between preferential pathways and surrounding matrix, a numerical model was constructed. The model was a two-dimensional representation of the unsaturated and shallow saturated zones created using the FRAC3DVS Version 3.40 code developed by Therrien and Sudicky (1996). This code can simulate three-dimensional fluid flow and transport under variably saturated situations in fractured, porous materials.

The model was set up to simulate geologic conditions surrounding SW-1. The model domain is 20 cm in the *x*-direction and 250 cm in the *z*-direction (Fig. 7). The upper 25 cm were given properties to simulate the stormflow zone. Physical properties, pressure/saturation, and saturation/hydraulic conductivity relationships were entered in tabular form from data by Wilson et al. (1992) and Rothschild et al. (1984). A mobile/immobile zone approach was used to simulate flow and transport in the stormflow zone. In this approach, flow is calculated based on the hydraulic conductivity of the bulk material. Transport is calculated based on the concept of two (mobile and immobile) overlapping continua. During transport, the calculated flow is channeled through the mobile zone and solutes are exchanged with the immobile zone through a transfer coefficient. Commonly, the mobile zone porosity is only a few percent of the total porosity. For this site, the macro- and mesopores, estimated to be between 1 and 5% of the total porosity, are considered to make up the mobile zone. No estimates were available for the first order transfer coefficient of mass between the two zones. To obtain a transfer coefficient, a search of the literature was conducted to ascertain a plausible range of coefficient values. A number of model runs were made varying the mobile zone porosity and transfer coefficient within the plausible range of each variable. The combination of mobile zone porosity and transfer coefficient which best fit the field data was selected for use in all future model runs.

The lower 225 cm were assigned properties of the saprolite. The saprolite was modeled as a porous media with a single vertical fracture, 100 μm in width, running the entire depth of the saprolite. Numerous investigations on the ORR (Solomon et al., 1992; Wilson et al., 1993) have concluded that bedding plane fractures in the saprolite control flow and transport in the unsaturated saprolite. In the study area, the geologic units are dipping at 45°. For this model, the fracture was modeled as vertical to simplify the numerical solution. The fracture aperture was chosen by assuming that the fractures constitute the bulk of macropores in the saprolite. Fracture spacing estimates of Drier et al. (1987), along with the percent of macroporosity, were used arrive at an estimate for fracture aperture.

A second-type (specified flux) condition was used for the upper boundary. A flux of 4 cm/day was used to simulate rain and zero flux to simulate drying. The sides of the domain were set at zero flux. A first-type (specified head) boundary condition set at 0.0 pressure head was used for the bottom boundary. The initial conditions were set by repeated cycles of wetting and drying until the head and saturation at the beginning of subsequent cycles did not change.

Fig. 6. Variations in $\delta^{18}O$ in the stormflow zone and shallow groundwater for a storm event in April–May, 1998. (a) Precipitation falling during the storm event in mm. (b) The $\delta^{18}O$ composition of water in the stormflow zone remains relatively constant, but is different than that of precipitation. The lack of variability in $\delta^{18}O$ is thought to be due to a relatively low precipitation rate that results in greater exchange with the micropores. (c) In the vicinity of SW-1, the $\delta^{18}O$ signal from the storm event is only seen close to the water table. A greater thickness of unsaturated saprolite at this location results in greater mixing between pre-event and event water as well as increased temporary storage of water in the unsaturated zone resulting in less recharge to the water table during the monitoring period. (d) In SW-3, the $\delta^{18}O$ response to the storm event is rapid at the water table and delayed at depth below the water table. The decreased thickness of unsaturated saprolite compared to the area around SW-1 results in less dilution of the storm signal as it passes through the unsaturated zone and greater penetration of the signal below the water table.

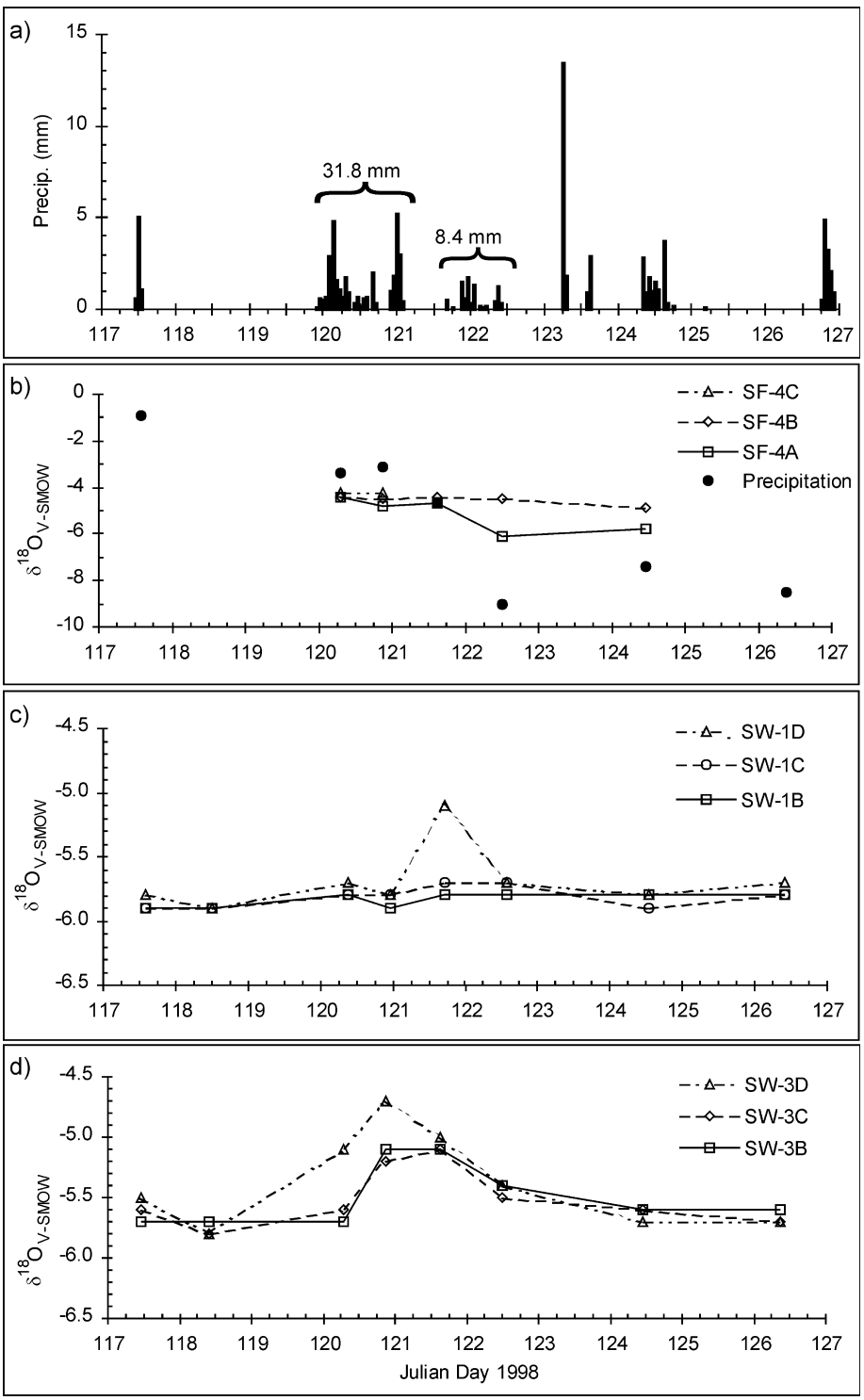
a)
Precip. (mm)
31.8 mm
8.4 mm
b)
SF-4C
SF-4B
SF-4A
Precipitation
δ18OV-SMOW
c)
SW-1D
SW-1C
SW-1B
δ18OV-SMOW
d)
SW-3D
SW-3C
SW-3B
δ18OV-SMOW
Julian Day 1998

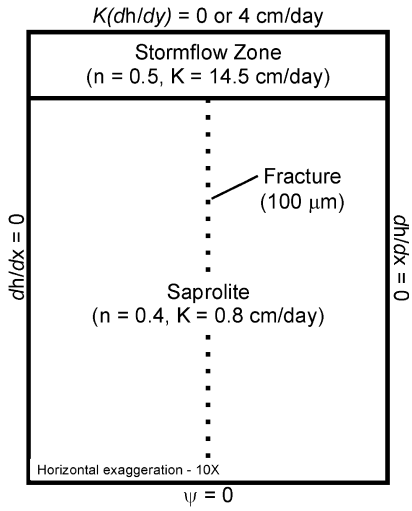

Fig. 7. Physical properties and boundary conditions for the numerical model.

The model was calibrated to the $\delta^{18}O$ data of the April–May, 1998 storm event at SW-1. Despite the simplifications of a vertical fracture representation and a constant precipitation rate, the model was able to provide a reasonable match for the timing and $\delta^{18}O$ value of the recharge recorded at the water table.

5. Modeling results

Two consecutive cycles of wetting and drying were simulated. Initially, a $\delta^{18}O$ of $-3‰$ was assigned to water throughout the model domain. The first cycle consisted of precipitation with a $\delta^{18}O$ of 0‰ for 1 day followed by 6 days of drying. The saturation conditions and $\delta^{18}O$ content of water at the end of the first cycle were saved and used as the initial conditions for the second cycle. The bulk $\delta^{18}O$ at the beginning of the second cycle is $-2.8‰$. The second cycle was identical in terms of the timing of precipitation and drying; however, the precipitation had a $\delta^{18}O$ of $-6‰$. At specified time steps throughout the simulation, the $\delta^{18}O$ content at selected nodes along the fracture and at various distances into the matrix were recorded. In addition, the $\delta^{18}O$ and volume of water crossing the upper and lower boundaries and the bulk $\delta^{18}O$ in the domain was also recorded.

To help in interpreting of the variations in $\delta^{18}O$, it is useful to first discuss the flow of water between the fracture and matrix during periods of wetting and drying. At the onset of precipitation, water is drawn into the top of the fracture at the boundary with the stormflow zone. After traveling only a short distance down the fracture, the water encounters a large saturation gradient with the surrounding matrix and is imbibed into the matrix (Fig. 8(a)). After precipitation stops and the system begins to dry, the direction of flow reverses and is from the matrix into the fracture throughout the entire domain (Fig. 8(b)). However, the saturation gradient between the matrix and fractures is smaller than during wetting, and as a result the magnitude of the drying vectors are several times smaller than the magnitude of the wetting vectors and the vectors have a larger vertical component during drying.

The field data for the several storm events indicates that there is significant temporal and spatial variability in $\delta^{18}O$. The model allows us to investigate this variability at much higher temporal and spatial resolution than is possible with field data. On Fig. 9, depth profiles of $\delta^{18}O$ in the fracture and 0.05, 0.4, and 0.9 cm into the matrix are plotted at various times over the course of the 14 day simulation.

The greatest amount of spatial variability is seen during periods of precipitation (Fig. 9(a) and (d), 1 day after the start of the simulated rain events). There is variability in $\delta^{18}O$ of water at all distances from the fracture and with depth at each distance from the fracture. The $\delta^{18}O$ in the fracture and 0.1 cm into the matrix are close to the value of precipitation, whereas, the $\delta^{18}O$ at 0.9 cm from fracture has changed little from the initial conditions. As the system begins to dry out (Fig. 9(b) and (e), 2 days after the end of the simulated rain events), spatial variability decreases significantly. Water within 0.4 cm of the fracture retains the $\delta^{18}O$ signature of the precipitation event, while the water at 0.9 cm has changed little from the initial conditions. Towards the end of the drying cycle (Fig. 9(c) and (f), 6 days after the end of the simulated rain events), the $\delta^{18}O$ of water within 0.05 cm of the fracture is nearly identical to that in the fracture and still retains the $\delta^{18}O$ signature of the precipitation event. The $\delta^{18}O$ of water 0.9 cm from the fracture still remains close to the initial value of $-3‰$.

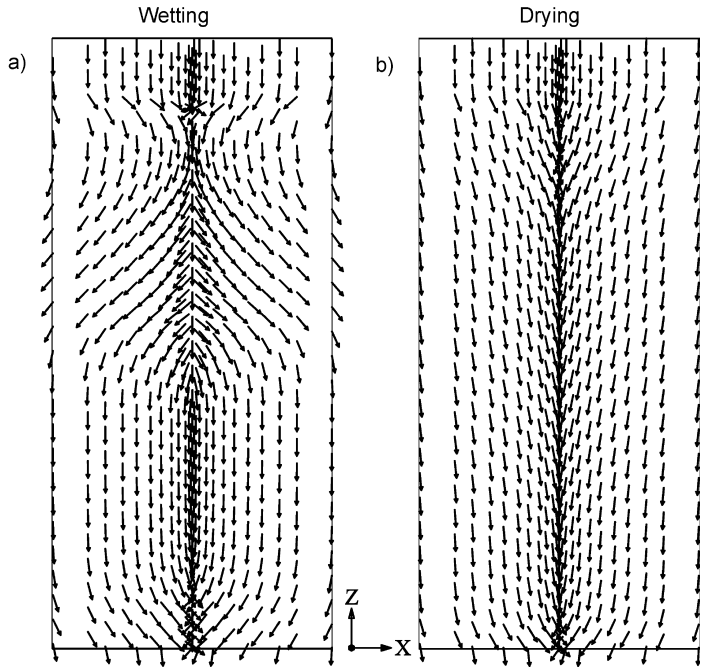

Fig. 8. Unscaled vectors indicating direction of advective flux of water during periods of wetting and drying of the unsaturated zone. (a) During wetting, water from the stormflow zone is drawn into the top of the fracture, saturating the fracture. The water then flows vertically down the fracture as well as horizontally into the surrounding matrix, which is unsaturated. (b) During drying, the fracture/matrix flow direction reverses so that water is drawn back into the fracture and rapidly transported vertically towards the water table.

It is interesting to note that despite advection being the dominant transport process in the vadose zone, the $\delta^{18}O$ of water 0.9 cm from the fracture does not significantly respond to the first storm event until nearly 7 days after the start of rain (Fig. 9(c)). The $\delta^{18}O$ at 0.9 cm continues to increase for several days (Fig. 9(d) and (e)) after the start of the second precipitation event with a $\delta^{18}O$ of $-6‰$. At the end of the simulation (Fig. 9(f), Day 14), the $\delta^{18}O$ at 0.9 cm is greater than the initial value of $-3‰$ despite the addition of equal amounts of 0 and $-6‰$ water crossing the upper boundary. This supports the field observations of the $\delta^{18}O$ of precipitation falling during a storm event influencing the $\delta^{18}O$ of water in the subsurface during the next storm event.

The influence of the previous storm event can also be illustrated by performing a hydrograph separation of the outflow of the model. For the purpose of discussion, the water exiting the bottom of the domain is imagined to be discharging into a stream. We recognize that the construction of the modeling domain does not accurately represent the hydrologic setting adjacent to a stream. However, geologic materials adjacent to streams have been shown to have preferential pathways. Soil scientists have long recognized that soil structure (peds and interpedal voids) results in preferential flow paths (Vervoort et al., 1999). Bioturbation (root channels and worm holes) also enhances preferential flow paths. On the ORR, Mulholland et al. (1990) conclude that preferential flow is important in generating stream flow during storm events. Although the physical process creating preferential flow paths may different than the fracture that the model represents, we believe that the model is representative of processes occurring in any type of preferential flow path. Therefore, the results of this simulation are relevant with respect to the assumptions inherent in the mass balance approach to hydrograph separation.

The mass balance Eqs. (1) and (2) can be used to calculate the amount of 'new' and old water in the stream. By setting:

$$R = Q_o/Q_s \tag{3}$$

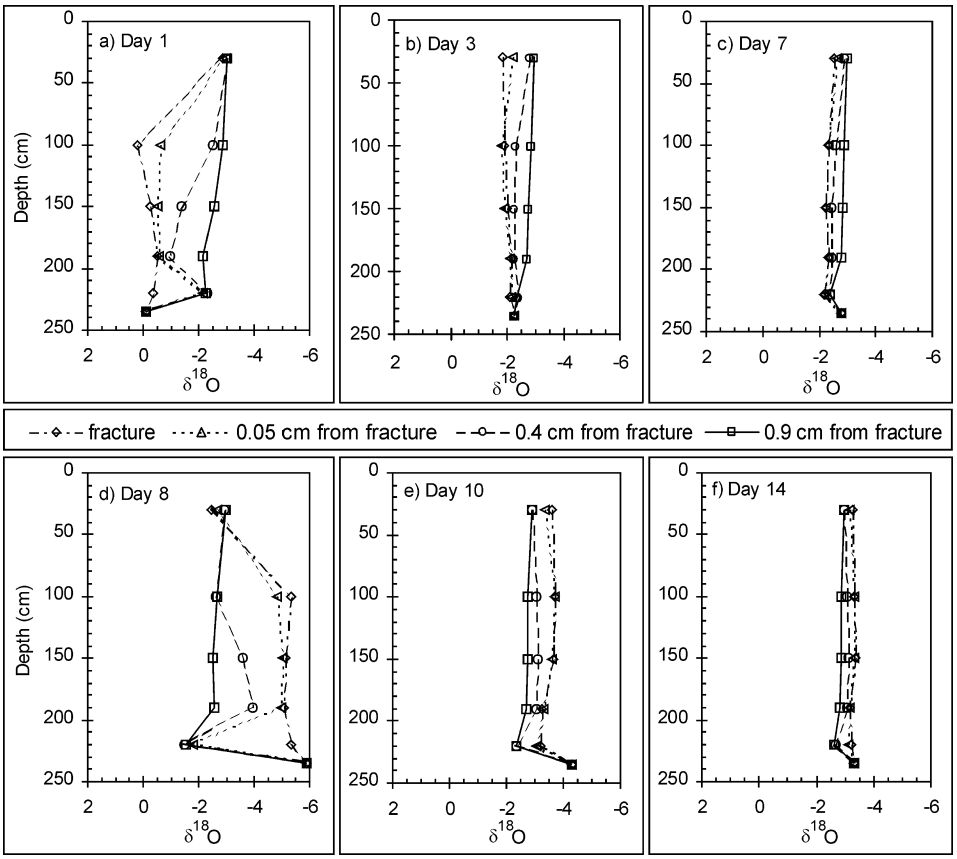

Fig. 9. Variations in $\delta^{18}O$ in a fracture and at several distances from the fracture in response to two model precipitation events. (a) At the end of 1 day of precipitation, $\delta^{18}O$ is variable at all depths and distances from the fracture. (b) After 2 days of drying, spatial variability in $\delta^{18}O$ has decreased, but the effects of the storm event have not propagated to a distance of 0.9 cm from the fracture. (c) After 6 days of drying, there is little spatial variability in $\delta^{18}O$ within 0.4 cm of the fracture and storm event changes are beginning to occur at 0.9 cm from the fracture. (d) After 1 day of rain at the start of the second storm event, $\delta^{18}O$ is variable at all depths and distances from the fracture. The $\delta^{18}O$ at 0.9 cm is still increasing, indicating that this distance from the fracture is still responding to the first storm event. (e) After 2 days of drying, spatial variability in $\delta^{18}O$ has decreased, but the effects of the second storm event have not propagated to a distance of 0.9 cm from the fracture. (f) After 6 days of drying, there is only minor spatial variability within 0.4 cm of the fracture, and the $\delta^{18}O$ at 0.9 cm has decreased slightly in response to the second storm event.

and substitution of Eq. (3) into Eq. (1) and followed by substitution of Eq. (1) into Eq. (2) yields:

$$R = (C_s - C_n)/(C_o - C_n) \quad (4)$$

Assuming that C_s is the $\delta^{18}O$ of water crossing the lower boundary of the model domain, the other $\delta^{18}O$ values are known and R can be calculated for each time step. For the first 7 day cycle, C_o (water in the model subsurface prior to the storm event) is $-3‰$ and C_n (the $\delta^{18}O$ of precipitation) is $0‰$. For the second 7 day cycle, C_o is $-2.8‰$ and C_n is $-6‰$. Using these values, the discharge of old water is plotted with the total discharge for the 14 day period (Fig. 10). During the first 7 day cycle, old water makes up all of the outflow for most of the first day. The percentage of old water then rapidly decreases as new precipitation begins to dominate discharge through the fracture, dropping to a value of 30% of the total discharge half way through Day 1. As the total discharge begins to decrease, the percentage of old water rapidly and then more gradually increases, reaching about 95% at the start of Day 7.

One might expect that the variations in percent old water would be similar in the second 7 day cycle since

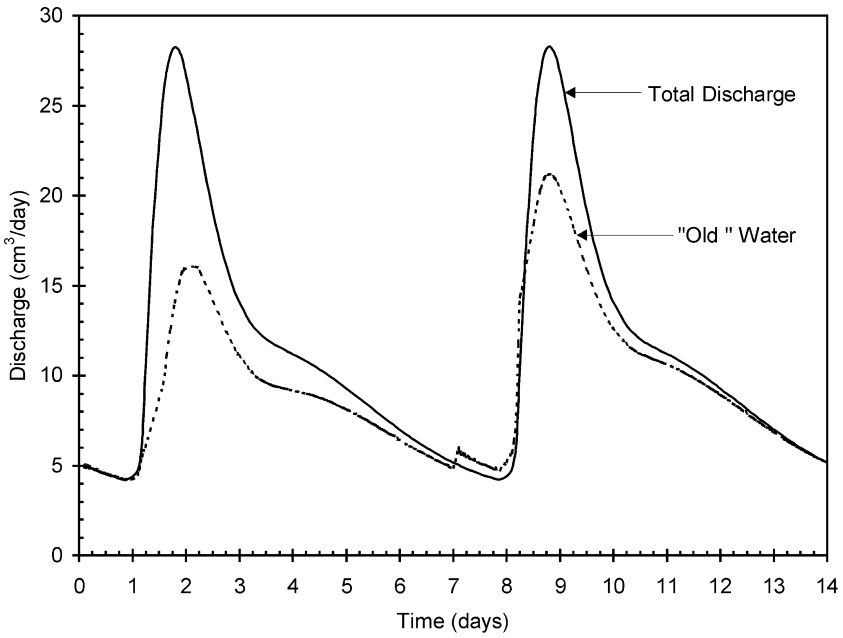

Fig. 10. Modeled total discharge and old water discharge for two consecutive storm events. Even though the initial conditions for each storm event are very similar, there is a greater percentage of calculated old water during the second event. The difference is a result of water in and around the fracture, which contributes to most of the flow out of the domain, that has a $\delta^{18}O$ which retains the signal from the first event and that is significantly different than the bulk value. At the beginning of Day 7, the sudden increase of old water discharge to greater than the total discharge is not physically realistic and results from a change in the values of C_o and C_n (see text for more detailed explanation).

the magnitude of the difference in $\delta^{18}O$ between C_o and C_n is very similar to the first 7 day cycle, only the sign is different. Note that the total discharge for the two cycles is identical and that the pattern of variation for the old water discharge is similar, however, the calculated magnitude of the old water discharge is different. The calculated discharge of old water suddenly jumps to a value greater than the total discharge at the start of Day 7. This, of course, is not real, but results from the change in the values of C_o and C_n. C_o has been recalculated to reflect the new bulk value of $\delta^{18}O$ for the entire model domain ($-2.8‰$) and the value for C_n is $-6‰$. The discharge from the domain is dominated by flow through the fracture, which stills retains the signal from the previous event ($\delta^{18}O$ greater than the bulk value), resulting in a calculated old water discharge greater than the total discharge. This situation persists into Day 8 before the percentage of old water drops to about 75% of the total discharge around the start of Day 9. Throughout the rest of the cycle, the discharge of old water gradually increases and is 100% of the discharge at Day 14.

Even though initial saturation conditions and the absolute difference between C_o and C_n were similar for the two cycles, the calculated magnitude of old water discharge was different. This is a result of using a bulk value for C_o. A closer match between the two cycles would have been obtained if only the $\delta^{18}O$ for the 0.5 cm surrounding the matrix had been used for the estimate of C_o. In theory, this is a more satisfying approach, but in reality, it is a very difficult to sample only water within 0.5 cm of a fracture. However, it clearly illustrates that the $\delta^{18}O$ of the previous storm event can have a significant influence on quantitative hydrograph separation.

6. Discussion

In the absence of an overland flow, almost all newly fallen precipitation must follow a flow path that bypasses the bulk of water in the subsurface in order for the precipitation signal to be seen in a stream. Preferential flow paths are present in many soil and

geologic settings. Some common examples are fractures in rocks, the space between soil peds, or sediments deposited in fluvial and glacial settings where there is vertical and discontinuous stratification of hydraulic conductivity. In all of these settings, the majority of transport will occur along the preferential pathways and the bulk of the surrounding matrix will be isolated from these pathways on time scales of a storm event (hours to days).

The field data presented in Section 4 demonstrate that there can be considerable spatial and temporal variability in $\delta^{18}O$ composition of water in the subsurface over the course of a storm event. Although the reservoir may be large (in this case a matrix porosity of 40–50%), the effect of preferential pathways greatly reduces the effective reservoir size on the time scale of a storm event. The storm event data shown on Figs. 4 and 6 indicate that the $\delta^{18}O$ composition of water in the stormflow zone changes over the course of the storm event. Both advective and diffusive mixing of precipitation and water already present in the stormflow zone continually alter the $\delta^{18}O$ composition of water that is ultimately transmitted to the water table.

As the January, 1998 storm (Fig. 4) illustrates, it is important to know the $\delta^{18}O$ of the previous storm event in order to interpret changes in the signal observed in the subsurface. During this storm event, the initial $\delta^{18}O$ of water in the stormflow zone and shallow groundwater (-8 to -9‰) are considerably more negative than precipitation and deeper groundwater (-4 to -6‰). Although the snowfall a week prior to this event was not sampled, it is hypothesized to be the cause of the anomalously negative $\delta^{18}O$ values in the shallow subsurface.

The January 1998 storm event data also demonstrate spatial heterogeneity in the isotopic composition of water in the stormflow zone prior to the start of precipitation. We can use mass balance calculations to illustrate the heterogeneity. The amount of water in the snowfall was only about 2% of the amount of water stored in the first meter of the subsurface. The tipping bucket rain gauge at site measured 0.63 cm of precipitation from the melting snow, and the total volume of water in the upper 1 m of the subsurface is estimated to have been 36 cm^3 per unit surface area. The subsurface volume of water was estimated from unpublished tensiometer data for the site and pressure/saturation data from Wilson et al. (1993) and Rothschild et al. (1984). The $\delta^{18}O$ of water in the stormflow zone during the initial stages of saturation was about -10‰. For the mass balance calculation, we assume that the $\delta^{18}O$ of water in the upper 1 m was constant value of -6‰ prior to the snowfall and the melting snow mixed completely with the water already in the upper 1 m. Using these assumptions, the $\delta^{18}O$ of the snowfall would have to have been around -238‰ (an unrealistic value) in order to decrease the $\delta^{18}O$ from -6 to -10‰ at the start of the January, 1998 event. However, using the same assumptions except that the water from snow melt only mixed with a small fraction (2%) of the total water in the upper 1 m yields a reasonable $\delta^{18}O$ value for the snow (-14.5‰). These simple calculations indicate that water from the melting snow had not mixed with the bulk of water in the upper 1 m after a period of 7 days.

With the numerical model, details of flow and transport between the fractures and matrix can be explored. The numerical model confirms that advection is the dominant transport process in the unsaturated zone. Even though advection is the most important process, the $\delta^{18}O$ of water in the matrix at a distance of greater than 0.4 cm from a fracture is not similar to the $\delta^{18}O$ of water in the fracture at any time after the start of the simulation (Fig. 9(a)–(f)). On a time scale of less than a day, there is a significant difference between the $\delta^{18}O$ of water in the fracture and $\delta^{18}O$ of water 0.1 cm into the matrix. This model suggests that for fracture (or preferential pathways) spacing >1 cm, there is spatial variability in the $\delta^{18}O$ content of the unsaturated zone on the time scale of 7 days. This interpretation is consistent with field observations at the site.

The field data from the shallow saturated zone also indicate spatial and temporal variability in $\delta^{18}O$ in this reservoir. Whereas, advection was the dominant solute exchange process between fractures and matrix in the unsaturated saprolite, diffusion is most likely the dominant process in the saturated saprolite. Although saturated zone modeling was not performed in this study, numerous other field and modeling studies have concluded that diffusion is the main mechanism of exchange of solutes between the fractures (or preferential pathways) and the surrounding matrix in saturated settings (Maloszewski and

Zuber, 1985). Given that diffusion is a slower mixing process than advection, spatial variability in $\delta^{18}O$ in water in the saturated zone would be expected for fracture spacing of ≥ 1 cm on storm event time scales.

The example of the modeled hydrograph separation takes a very simplistic view of stream flow generation during storm events. However, we think it illustrates how errors resulting from the assumptions used in mass balance hydrograph separation might occur in settings dominated by preferential flow paths. Preferential flow paths in geologic materials are more likely to be the rule than the exception in the shallow subsurface that generates stream flow. Soil scientists have long recognized flow and transport in soils is dominated by preferential flow paths. Soils are often structured, with coherent aggregates of soil particles (peds) separated by voids. These are analogous to fractures in rocks or saprolite. In addition to structure, bioturbation (root channels and worm holes) creates additional preferential flow paths in soils. On a larger scale, sediments in stream valleys are highly heterogeneous. A cross-section through a floodplain might reveal alternating layers of silt, channel sand and gravel, or colluvium from adjacent hillslopes, in layers form millimeters to meters thick.

Given the likelihood of preferential flow paths in geologic materials adjacent to streams, the assumption of a constant composition of the subsurface reservoir is questionable. The validity of the assumptions inherent in mass balance storm hydrograph separation has been questioned by other researchers, and has led to refinements in the mass balance technique (Harris et al., 1995) and to quantification of the uncertainty due to natural variability and analytical error in measurement of the composition of various reservoirs (Genereux, 1998). We believe that the field observations and numerical modeling described here offer another approach to quantitative storm hydrograph separation. Field investigations for storm hydrograph separation should be designed to take into account spatial and temporal variability due to preferential flow. Such investigations would provide conceptual models for more realistic numerical models that explicitly represent preferential flow. Such a numerical model may not be possible at the watershed scale due to the enormity of data collection as well as computational resources. However, at the subwatershed scale or a two-dimensional cross-section from hillslope to stream would result in valuable insight into spatial and temporal scales of importance for storm hydrograph separation.

7. Conclusions

Mass balance calculations using environmental tracers to separate hydrographs into different components is very appealing because of its simplicity. In order to use mass balance equations, a number of assumptions must be shown to be valid, including a constant and known concentration of a chemical tracer in soil moisture and groundwater.

Field data from a site with preferential pathways (relict fractures in a sedimentary rock saprolite) indicate considerable temporal and spatial variability in $\delta^{18}O$ in the subsurface on the time scale of a storm event. The field data indicate that there is limited mixing between the water flowing in the relict fractures and water in the surrounding permeable matrix. The implication for hydrograph separation is that a measurement of soil moisture $\delta^{18}O$ which represent a bulk value may be in error since the only water from the matrix a short distance from the fracture actually contributes to flow in the fracture.

The results of numerical modeling support the interpretations of the field data. The numerical model shows that there is an advective flux from the fractures into the matrix during wetting and a reversal of the flux direction during drying. $\delta^{18}O$ depth profiles at various distances from the fracture indicate that the influence of advective mixing rapidly decreases away from the fracture. These depth profiles also suggest that the $\delta^{18}O$ of the previous storm has a significant influence on the $\delta^{18}O$ in preferential pathways in subsequent storm events.

To further illustrate the influence of prior storm events, hydrograph separation mass balance equations were applied to the model outflow. The percentage of old water in the model discharge was calculated for two successive storm events. Despite similar initial conditions and input signals, the percent old water in the discharge was different for the two events. The difference was attributed to the $\delta^{18}O$ signature of the first storm that was still present in the matrix immediately surrounding the fracture, which was different than bulk value for the entire domain. The

bulk value that is used in the mass balance calculations and results is differences in the percent old water during the second storm event.

These observations, interpretations and modeling results cast further doubt on the use of mass balance equations to quantitatively separate hydrographs. We suggest that quantitative hydrograph separation can only be accomplished by conducting detailed investigation of subsurface flow and transport, and the use of calculations other than steady state mass balance equations. We present an approach that uses numerical modeling to explore the interaction of water and solutes between preferential pathways and the surrounding lower permeability matrix. To our knowledge, this approach has not been applied to the problem of hydrograph separation. We believe that future investigations designed to collect data appropriate for use in this type of modeling approach will significantly enhance our ability to quantitatively separate the various components that contribute to stream flow during storm events.

Acknowledgments

This research was funded in part by a research fellowship to the first author from Oak Ridge National Laboratory, Environmental Sciences Division that was administered by Oak Ridge Associated Universities. Special thanks to G. Moline for providing access to field and laboratory equipment, assistance in field sampling, and overall guidance of the field work, and N. Farrow for his creative abilities with well installation and sampling. This manuscript benefited significantly from the comments of two reviewers.

References

DeWalle, D.R., Swistock, B.R., Sharpe, W.E., 1988. Three component tracer model for stormflow on a small Appalachian forested catchment. Journal of Hydrology 104, 301–310.

Drier, R.B., Solomon, D.K., Beaudoin, C.M., 1987. Fracture characterizations in the unsaturated zone of a shallow land burial facility. American Geophysical Monograph 42, 51–59.

Elsenbeer, H., West, A., Bonell, M., 1994. Hydrologic pathways and stormflow hydrochemistry at South Creek, northeast Queensland. Journal of Hydrology 162, 1–21.

Genereux, D., 1998. Quantifying uncertainty in tracer-based hydrograph separations. Water Resources Research 34, 915–919.

Genereux, D., Hemond, H.F., Mulholland, P.J., 1993. Use of radon-222 and calcium as tracers in a three-end-member mixing model for streamflow generation on the West Fork of Walker Branch watershed. Journal of Hydrology 142, 167–211.

Harris, D.M., McDonnell, J.J., Rodhe, A., 1995. Hydrograph separation using continuous open system isotope mixing. Water Resources Research 31, 157–171.

Kendall, C., McDonnell, J.J., 1993. Effect of intrastorm isotopic heterogeneities of rainfall, soil water, and groundwater on runoff modeling. In: Peters, N.E., Walling, D.E., Hoehn, E., Leibundgut, C., Tase, N. (Eds.), Tracers in Hydrology. Proceedings of the Yokohama Symposium, July 1993, IAHS Publ. No. 215, pp. 41–48.

Luxmoore, R.J., 1981. Micro-, meso-, and macroporosity of soil. Soil Science Society of America Journal 45, 671–672.

Luxmoore, R.J., Jardine, P.M., Wilson, G.V., Jones, J.R., Zelazny, L.W., 1990. Physical and chemical controls of preferred path flow through a forested hillslope. Geoderma 46, 139–154.

Maloszewski, P., Zuber, A., 1985. On the theory of tracer experiments in fissured rocks with a porous matrix. Journal of Hydrology 79, 333–358.

McKay, L.D., Driese, S.G., 1999. Influence of pore structure on groundwater flow and contaminant transport in mudrock saprolite, Oak Ridge, TN. Geological Society of America Annual Meeting Abstracts with Programs 31, A449–A450.

Mulholland, P.J., 1993. Hydrometric and stream chemistry evidence of three storm flowpaths in Walker Branch watershed. Journal of Hydrology 151, 291–316.

Mulholland, P.J., Wilson, G.V., Jardine, P.M., 1990. Hydrogeochemical response of a forested watershed to storms: effects of preferential flow along shallow and deep pathways. Water Resources Research 26, 3021–3036.

O'Brien, C., Hendershot, W.H., 1993. Separating streamflow into groundwater, solum and upwelling flow and its implications for hydrochemical modelling. Journal of Hydrology 146, 1–12.

Pilgram, D.H., Huff, D.D., Steele, T.D., 1979. Use of specific conductance and contact time relations for separating flow components in storm runoff. Water Resources Research 15, 329–339.

Pinder, G.F., Jones, J.F., 1969. Determination of the ground-water component of peak discharge from the chemistry of total runoff. Water Resources Research 5, 438–455.

Rothschild, E.R., Huff, D.D., Spalding, B., 1994. Characterization of soils at proposed Solid Waste Storage Area (SWSA) 7, ORNL/TM-9326, Oak Ridge National Laboratory, Oak Ridge, TN.

Sklash, M.G., Farvolden, R.N., 1979. The role of groundwater in storm runoff. Journal of Hydrology 43, 45–65.

Sklash, M.G., Farvolden, R.N., 1982. The use of environmental isotopes in the study of high-runoff episodes in streams. In: Perry, E.C. Jr., Montgomery, C.W. (Eds.), Isotope Studies of Hydrologic Processes, Northern Illinois University Press, Dekalb, IL, pp. 65–73.

Solomon, D.K., Moore, G.K., Toran, L.E., Dreier, R.B., McMaster,

W.M., 1992. Status report: a hydrologic framework for the Oak Ridge Reservation, ORNL/TM-12026, Oak Ridge National Laboratory, Oak Ridge, TN.

Stewart, M.K., McDonnell, J.J., 1991. Modeling base flow soil water residence times from deuterium concentrations. Water Resources Research 27, 2681–2693.

Therrien, R., Sudicky, E.A., 1996. Three-dimensional analysis of variably-saturated flow and solute transport in discretely-fractured porous media. Journal of Contaminant Hydrology, 23, 1–44.

Van der Hoven, S.J., 2000. Using natural tracers to evaluate flow and transport in saprolite and fractured sedimentary rocks. PhD Dissertation, University of Utah, p. 128.

Vervoort, R.W., Radcliffe, D.E., West, L.T., 1999. Soil structure development and preferential solute flow. Water Resources Research 35, 913–928.

Watkins, D.R., Ammons, J.T., Branson, J.L., Burgoa, B.B., Goddard, P.L., Hatmaker, T.L., Hook, L.A., Jackson, B.L., Kimbrough, C.W., Lee, S.Y., Lietzke, D.A., McGinn, C.W., Nourse, B.D., Schmoyer, R.L., Stinnette, S.E., Switek, J., 1993. Final report on the background soil characterization project at the Oak Ridge Reservation, Oak Ridge, Tennessee, Volume 2-Data, DOE/OR/01-1175/V2, Oak Ridge National Laboratory, Oak Ridge, TN.

Watson, K.W., Luxmoore, R.J., 1986. Estimating macroporosity in a forested watershed by use of a tension infiltrometer. Soil Science Society of America Journal 50, 578–582.

Wilson, G.V., Jardine, P.M., Luxmoore, R.J., Jones, J.R., 1990. Hydrology of a forested hillslope during storm events. Geoderma 46, 119–138.

Wilson, G.V., Jardine, P.M., Luxmoore, R.J., Zelazny, L.W., Todd, D.E., 1991a. Hydrogeochemical processes controlling subsurface transport from an upper subcatchment of Walker Branch watershed during storm events. 1. Hydrologic transport processes. Journal of Hydrology 123, 297–316.

Wilson, G.V., Jardine, P.M., Luxmoore, R.J., Zelazny, L.W., Todd, D.E., Lietzke, D.A., 1991b. Hydrogeochemical processes controlling subsurface transport from an upper subcatchment of Walker Branch watershed during storm events. 2. Solute transport processes. Journal of Hydrology 123, 317–336.

Wilson, G.V., Jardine, P.M., Gwo, J.P., 1992. Modelling the hydraulic properties of a multi region soil. Soil Science Society of America Journal, 56, 1731–1737.

Wilson, G.V., Jardine, P.M., O'Dell, J.D., Collineau, M., 1993. Field-scale transport from a buried line source in variably saturated soil. Journal of Hydrology 145, 83–109.